

This is a repository copy of *Structure of micro-instabilities in tokamak plasmas: Stiff transport or plasma eruptions?*.

White Rose Research Online URL for this paper:

<https://eprints.whiterose.ac.uk/id/eprint/85081/>

Version: Published Version

Article:

Dickinson, D., Roach, C. M., Skipp, J. M. et al. (1 more author) (2014) Structure of micro-instabilities in tokamak plasmas: Stiff transport or plasma eruptions? *Physics of Plasmas*, 21 (1). 010702. ISSN 1070-664X

<https://doi.org/10.1063/1.4861628>

Reuse

Items deposited in White Rose Research Online are protected by copyright, with all rights reserved unless indicated otherwise. They may be downloaded and/or printed for private study, or other acts as permitted by national copyright laws. The publisher or other rights holders may allow further reproduction and re-use of the full text version. This is indicated by the licence information on the White Rose Research Online record for the item.

Takedown

If you consider content in White Rose Research Online to be in breach of UK law, please notify us by emailing eprints@whiterose.ac.uk including the URL of the record and the reason for the withdrawal request.

Structure of micro-instabilities in tokamak plasmas: Stiff transport or plasma eruptions?

D. Dickinson, C. M. Roach, J. M. Skipp, and H. R. Wilson

Citation: *Physics of Plasmas* (1994-present) **21**, 010702 (2014); doi: 10.1063/1.4861628

View online: <http://dx.doi.org/10.1063/1.4861628>

View Table of Contents: <http://scitation.aip.org/content/aip/journal/pop/21/1?ver=pdfcov>

Published by the AIP Publishing

Articles you may be interested in

[On the non-stiffness of edge transport in L-mode tokamak plasmas](#)

Phys. Plasmas **21**, 055906 (2014); 10.1063/1.4876612

[Development of drift-resistive-inertial ballooning transport model for tokamak edge plasmas](#)

Phys. Plasmas **17**, 082511 (2010); 10.1063/1.3478979

[Blob birth and transport in the tokamak edge plasma: Analysis of imaging data](#)

Phys. Plasmas **13**, 092509 (2006); 10.1063/1.2355668

[Advances in measurement and modeling of the high-confinement-mode pedestal on the Alcator C-Mod tokamak](#)

Phys. Plasmas **13**, 056103 (2006); 10.1063/1.2180748

[Edge instability regimes with applications to blob transport and the quasicohherent mode](#)

Phys. Plasmas **12**, 092511 (2005); 10.1063/1.2048847



Structure of micro-instabilities in tokamak plasmas: Stiff transport or plasma eruptions?

D. Dickinson,^{1,2,a)} C. M. Roach,² J. M. Skipp,¹ and H. R. Wilson¹

¹York Plasma Institute, Department of Physics, University of York, Heslington, York YO10 5DD, United Kingdom

²EURATOM/CCFE Fusion Association, Culham Science Centre, Abingdon, Oxon OX14 3DB, United Kingdom

(Received 14 November 2013; accepted 20 December 2013; published online 8 January 2014)

Solutions to a model 2D eigenmode equation describing micro-instabilities in tokamak plasmas are presented that demonstrate a sensitivity of the mode structure and stability to plasma profiles. In narrow regions of parameter space, with special plasma profiles, a maximally unstable mode is found that balloons on the outboard side of the tokamak. This corresponds to the conventional picture of a ballooning mode. However, for most profiles, this mode cannot exist, and instead, a more stable mode is found that balloons closer to the top or bottom of the plasma. Good quantitative agreement with a 1D ballooning analysis is found, provided the constraints associated with higher order profile effects, often neglected, are taken into account. A sudden transition from this general mode to the more unstable ballooning mode can occur for a critical flow shear, providing a candidate model for why some experiments observe small plasma eruptions (Edge Localised Modes, or ELMs) in place of large Type I ELMs. [<http://dx.doi.org/10.1063/1.4861628>]

Micro-instabilities in magnetised plasmas are those with a characteristic length scale across magnetic field lines comparable to the ion Larmor radius, ρ_i . The particle drifts play a key role in the dynamics and, therefore, often characterise their growth rate, which is weak compared to Alfvénic modes. While these micro-instabilities are relatively benign, they are, nevertheless, important because they drive turbulence that degrades plasma confinement. Understanding turbulence and its influence on confinement is one of the key challenges facing magnetically confined fusion plasmas.

In this Letter, we consider the generic linear properties of micro-instabilities that drive turbulence in a toroidal magnetic confinement device, such as a tokamak. Our new 2D calculations of their eigenmode structure are compared with analytic ‘ballooning formalism’ approaches that reduce the problem to 1D.^{1,2} Ballooning models have identified two types of mode structures: (1) An *isolated* mode is the most unstable and is related to the conventional ballooning mode of ideal magnetohydrodynamics (MHD),^{3–6} but only exists in very special circumstances and (2) a more stable *general* mode that exists throughout the plasma. Both of these mode structures are found in our 2D eigenmode calculations, providing first quantitative numerical tests that confirm ballooning theory. Our results suggest a possible mechanism for a sudden transition from benign micro-instabilities driving turbulent transport to stronger instabilities that could release small filamentary eruptions and locally collapse the profiles. This mechanism may form the basis of a model for small Edge Localised Modes (ELMs) in tokamaks.⁸

While our results are generic to any micro-instability in a tokamak plasma, it is helpful to illustrate the analysis with a particular model. Thus, we consider a large aspect ratio, circular cross section tokamak equilibrium, with flux

surfaces labelled by the minor radius, r . We consider only electrostatic fluctuations and assume an adiabatic electron response. We solve the gyrokinetic equation for the ion distribution function, which is expanded assuming that the ion transit and drift frequencies are small compared to the mode frequency. For a wavelength across magnetic field lines that is larger than the ion Larmor radius, quasi-neutrality provides the following equation for the perturbed electrostatic potential, ϕ :⁹

$$\left[\rho_i^2 \frac{\partial^2}{\partial x^2} - \frac{\sigma^2}{\omega^2} \left(\frac{\partial}{\partial \theta} + ik_\theta \hat{s}x \right)^2 - \frac{2\epsilon_n}{\omega} \left(\cos \theta + \frac{i \sin \theta}{k_\theta} \frac{\partial}{\partial x} \right) - \frac{\omega - 1}{\omega + \eta_i} - k_\theta^2 \rho_i^2 \right] \phi(x, \theta) = 0, \quad (1)$$

where $\sigma = \epsilon_n / (qk_\theta \rho_i)$, \hat{s} is the magnetic shear, q is the safety factor, $\epsilon_n = L_n / R$, L_n is the density gradient scale length, R is the major radius, ω is the complex mode frequency normalised to the electron diamagnetic frequency, k_θ is the poloidal wave number, and η_i is the ratio of density to ion temperature gradient length scales, and we have assumed equal electron and ion temperatures. The poloidal angle, θ , is defined so that $\theta = 0$ at the outboard mid-plane and $x = r - r_s$ is the distance from the rational surface at $r = r_s$. The model is valid in the core relevant limit $\eta_i \gg 1$ which recovers the ion temperature gradient mode (ITG), which is our focus here.

The 2D eigenmode equation can be conveniently solved by adopting a Fourier transform representation of ϕ (Ref. 10)

$$\phi(x, \theta) = \int_{-\infty}^{\infty} A(\theta_0) \xi(\theta, \theta_0) \exp[inq'x(\theta_0 - \theta)] d\theta_0, \quad (2)$$

so that $nq'\theta_0$ can be interpreted as a radial wave-number at $\theta = 0$ (n is the toroidal mode number, $q' = dq/dr$, and $nq' = k_\theta \hat{s}$). The amplitude factor $A(\theta_0)$ is assumed to vary

^{a)}Electronic mail: dd502@york.ac.uk

faster with θ_0 than $\xi(\theta, \theta_0)$. Substituting Eq. (2) into Eq. (1) and following a procedure which extends that set out in Ref. 1 (and analysed in detail in Ref. 2), we can then reduce Eq. (1) to a sequence of 1D ordinary differential equations by expanding in n , which is assumed to be large. This yields to leading order the ballooning equation for $\xi(\theta, \theta_0)$

$$\left[\frac{\sigma^2}{\omega^2} \frac{d^2}{d\theta^2} + k_\theta^2 \rho_i^2 \hat{s}^2 (\theta - \theta_0)^2 + \frac{2\epsilon_n}{\omega} [\cos \theta + \hat{s}(\theta - \theta_0) \sin \theta] + \frac{\omega - 1}{\omega + \eta_i} - k_\theta^2 \rho_i^2 \right] \xi(\theta, \theta_0) = 0, \quad (3)$$

providing an eigenvalue condition that relates ω , θ_0 , and x written as $\omega = \Omega(x, \theta_0)$. $\Omega(x, \theta_0)$ is obtained by solving Eq. (3) numerically over all θ_0 for the range of interest in x , noting that the equilibrium parameters vary slowly with x . Restricting consideration to small x (anticipating modes localised about $r = r_s$), we can Taylor expand $\Omega = \Omega_0(\theta_0) + \Omega_x(\theta_0)x + [\Omega_{xx}(\theta_0)/2]x^2 + \dots$. Multiplying by ϕ and transforming into Fourier space, it is straightforward to show that $x\phi$ is proportional to $(i/nq')dA/d\theta_0$ and $x^2\phi$ to $-1/(nq')^2 d^2A/d\theta_0^2$, so we have

$$\frac{\Omega_{xx}(\theta_0)}{2(nq')^2} \frac{d^2A}{d\theta_0^2} - \frac{i\Omega_x(\theta_0)}{nq'} \frac{dA}{d\theta_0} + [\omega - \Omega_0(\theta_0)]A = 0. \quad (4)$$

It follows from Eq. (3) that $\xi(\theta, \theta_0) = \xi(\theta + 2l\pi, \theta_0 + 2l\pi)$ for any integer l , so from Eq. (2), ϕ is periodic in θ provided A is periodic in θ_0 . This provides the boundary condition that determines ω as an eigenvalue of Eq. (4). Solving for $A(\theta_0)$, together with $\xi(\theta, \theta_0)$, provides the 2D eigenfunction $\phi(x, \theta)$.

Analytically, we can deduce two types of solution from Eq. (4), which are the ‘isolated’ and ‘general’ modes of Ref. 1. The *isolated* mode exists at the special radial location where $\Omega_x = 0$; this is the classic ballooning mode originally derived for ideal MHD.^{3–6} $A(\theta_0)$ is highly localised around the θ_0 value where $\Omega_0(\theta_0)$ is stationary, say $\theta_0 = \theta_m$. Expanding about that position, Eq. (4) becomes a Hermite equation, with solution

$$A(\theta_0) = \exp \left[-\frac{nq'}{2} \left(\frac{\Omega_{\theta_0\theta_0}}{\Omega_{xx}} \right)^{1/2} (\theta_0 - \theta_m)^2 \right], \quad (5)$$

where the sign of the square root is chosen to give a bounded solution in θ_0 . $A(\theta_0)$ has a width $\sim n^{-1/2}$, justifying our Taylor expansion of $\Omega_0(\theta_0)$ about $\theta_0 = \theta_m$. The eigenvalue condition provides

$$\omega = \Omega_0(\theta_0 = \theta_m) - \frac{(\Omega_{xx}\Omega_{\theta_0\theta_0})^{1/2}}{2nq'} + \mathcal{O}(n^{-2}). \quad (6)$$

Note that the *isolated* mode growth rate is determined from the 1-D ballooning equation by evaluating the eigenvalue at the x and θ_0 values which maximise the growth rate. Furthermore, if $A(\theta_0)$ is highly localised, the Fourier transform of Eq. (2) will be dominated by the region around $\theta_0 = \theta_m$. This, together with the fact that $\xi(\theta, \theta_0)$ peaks close

to $\theta = \theta_0$, leads to an expression for the potential, ϕ which peaks at $\theta = \theta_m$. For our up-down symmetric model, $\theta_m = 0$, and an *isolated* mode will be localised on the outboard side of the tokamak.

To summarise, the *isolated* mode exists when $\Omega_x = 0$; one selects the value of θ_0 to maximise the growth rate, and the mode is localised about $\theta = \theta_0$, which is often at the outboard mid-plane. While this is intuitive from a physics point of view, if $\Omega_x \neq 0$ (which is usually the case), the constraints of the higher order theory do not allow such a mode to exist, as we now discuss.

In general, the first order radial derivative in Eq. (4) cannot be neglected. Often Ω_x is complex, and it can only be neglected when its real *and* imaginary parts vanish at the same value of x ; hence, the *isolated* mode only exists under very special situations. In the more general case with finite Ω_x , we can neglect the Ω_{xx} term of Eq. (4). Dividing the remaining terms by $A\Omega_x$ and integrating over a full period in θ_0 , we derive the eigenvalue condition $\omega = \langle \Omega_0 \Omega_x^{-1} \rangle / \langle \Omega_x^{-1} \rangle$, where angled brackets denote averaging over θ_0 . Substituting this value of ω into Eq. (4) and integrating yields the required periodic expression for $A(\theta_0)$. One finds that $A(\theta_0)$ is still localised in θ_0 , provided $\Omega(x, \theta_0)$ is complex, but now around the value of θ_0 where $\omega = \Omega_0(\theta_0)$; in our simple model, this position is typically at the top or bottom of the tokamak,⁷ corresponding to $\theta_0 = \pm\pi/2$. This *general* mode is more stable than the *isolated* mode, with a growth rate which is the average of Ω_0 over θ_0 rather than the maximum, and the mode sits away from the outboard mid-plane. Due to the difference in stability, the *general* mode will have a higher critical gradient than the *isolated* mode.

To provide quantitative numerical tests of this theory, we solve Eq. (3) for a specific parameter set: $n = 50$, $\hat{s} = 2$, $k_\theta \rho_i = 0.33$, $R/a = 10$, $q(r = r_s) = 1.8$, and $q(r) = 3.45(r/a)^2$. We further assume that all parameters in Eq. (1) are independent of x except for η_i . In this system, an *isolated* mode should exist if η_i has a maximum in x (as we shall illustrate), while a linear η_i profile should yield a *general* mode. For the various η_i profiles chosen, we fix $\eta_i = 5$ at $r = r_s$ giving the same local eigenvalue at $x = 0$, $\Omega(x = 0, \theta_0)$, for each case. While q is held constant in the co-efficients of Eq. (1), $\hat{s} \neq 0$ is required to provide a distribution of rational surfaces across the minor radius.

Figure 1 shows $\Omega(x, \theta_0)$ from solving Eq. (3) for two types of η_i profile: A quadratic profile peaking near the rational surface (Figures 1(a) and 1(b)), and one which decreases linearly in x (Figures 1(c) and 1(d)). Both exhibit $\Omega_0 \sim \cos \theta_0$, while Ω_x and Ω_{xx} are approximately independent of θ_0 .

For the peaked η_i profile, $\Omega_x = 0$ at $r = r_s$, and we expect an *isolated* mode. (This is a special situation: If we were to include radial variations in the other equilibrium parameters of our model then, even for the peaked η_i profile, the real and imaginary parts of Ω would not be stationary at the same x , and no position would exist where $\Omega_x = 0$.) The complex mode frequency from the 1D ballooning procedure is $\omega = -0.025 + i0.319$.

With the linear η_i profile, $\Omega(x, \theta_0)$ no longer has a maximum at $x = 0$. Employing the averaging procedure relevant

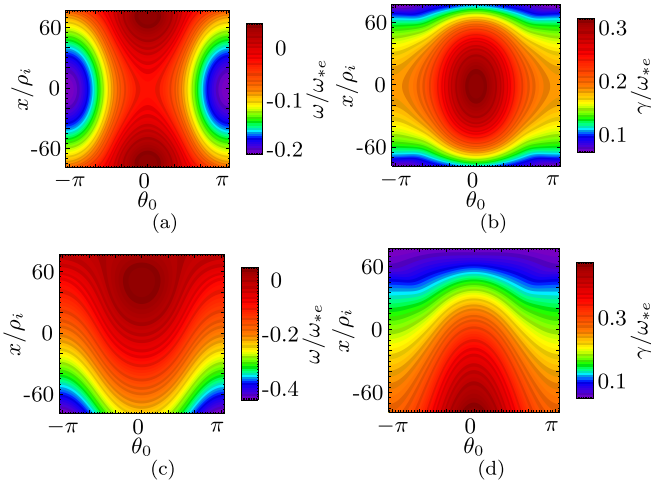


FIG. 1. Contours of the local frequency ((a) and (c)) and growth rate ((b) and (d)) as a function of x and θ_0 derived from the 1D ballooning code solution of Eq. (3) for the peaked and linear η_i profiles, respectively.

to the *general* mode, we obtain $\omega = -0.108 + i0.230$, revealing a substantially more stable situation than for the peaked η_i profile. Recall that in both cases the local equilibrium parameters are identical at $x=0$. Solving Eq. (4) for $A(\theta_0)$ with this *general* mode eigenvalue, we find that $\ln A(\theta_0) \sim \sin \theta_0$ (with a complex coefficient), so $A(\theta_0)$ is strongly peaked around $\theta_0 = \pi/2$. For our circular geometry, this results in a mode structure for $\phi(x, \theta)$ that is localised at the top of the plasma. Whether the localisation is at the top or bottom of the plasma depends upon the sign of $\Omega_{\theta_0}/\Omega_x$.

We test this generalised ballooning theory quantitatively using full 2D numerical solutions to Eq. (1). We first decompose $\phi(x, \theta)$ into poloidal Fourier harmonics, $\phi(x, \theta) = \sum_m u_m(x) \exp(im\theta)$, and then solve the set of coupled equations for the radial dependence of the coefficients, $u_m(x)$, to determine the complex mode frequency, ω , as an eigenvalue of the system. Radially localised modes are sought, and we therefore employ zero Dirichlet boundary conditions in the radial direction. The results for the two different eigenmode structures are shown in Figure 2. With the peaked η_i profile, the mode is indeed localised on the outboard side, while for the linear profile, it is peaked at the top of the plasma. We find no 2D eigenmode on the outboard side when the η_i profile is linear. These mode structures can also be obtained from the 1D ballooning procedure; we do not show them here because they are visibly indistinguishable from these 2D

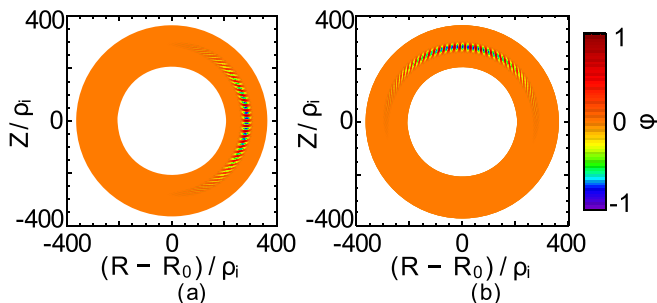


FIG. 2. 2D eigenmode structure for the potential ϕ ((a) and (b)) in the poloidal plane for the peaked and linear η_i profiles, respectively. The (orange) shaded region in the poloidal cross-section shows the simulation domain.

solutions. The eigenvalues from the 2D analysis are $\omega = -0.025 + i0.316$ and $\omega = -0.110 + i0.239$ for the peaked and linear η_i profiles, respectively. These results are in excellent agreement with the 1D ballooning analysis.

In Ref. 11, Kim and Wakatani argued that a continuum of modes can exist when $\Omega_x \neq 0$. However, these are not eigenmodes of the system. Such a continuum arises because there is a range of solutions to Eq. (4), which provide the desired localisation of $A(\theta_0)$ and hence the existence of the Fourier transform, Eq. (2). However, in general, those solutions do not provide a form for A that is periodic in θ_0 , which is required for ϕ to be periodic in θ . For this reason, the Kim-Wakatani modes are not physical eigenmodes, as was also noted in Ref. 12. We do not see Kim-Wakatani modes in our 2D eigenmode solutions, confirming the conclusions of Ref. 12.

We can use our 2D solutions to explore the relation between *isolated* and *general* modes. We start with an η_i profile which is peaked at $x=0$ so that the more unstable *isolated* mode exists. Adding a linear contribution to the η_i profile simply shifts the position of the maximum of η_i : The *isolated* mode still exists, but adjusts its position to sit at the point where η_i is a maximum. A more interesting situation arises when one introduces flow shear into the problem as this then shifts the position where the local frequency is stationary relative to that where the local growth rate peaks. No isolated mode is then possible. Thus in Eq. (1), we introduce a Doppler shift $\omega \rightarrow \omega + nq'\gamma_E x$, working in the rest frame of the rational surface. The shearing rate, $\gamma_E = d\Omega_\phi/dq$, parameterises the shear in the toroidal rotation, Ω_ϕ . Figures 3(a) and 3(b) show how the mode frequency and growth rate derived from 2D solutions respond to γ_E ; they are symmetric under $\gamma_E \rightarrow -\gamma_E$. Note how the *isolated* mode that exists at $\gamma_E = 0$, smoothly evolves into the *general* mode, as expected from analytic theory,^{2,13} for a relatively low value of $|\gamma_E| \sim 0.015 \ll \gamma$, where γ is the ITG growth rate. Thus, the

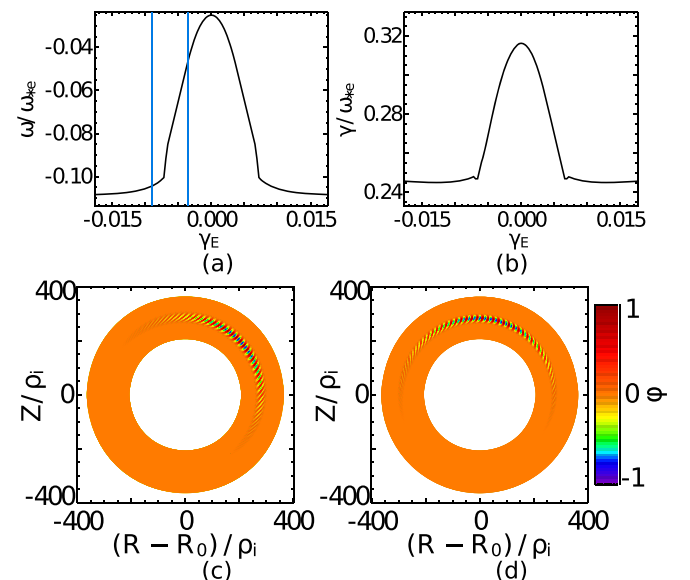


FIG. 3. The mode frequency and growth rate ((a) and (b)) as a function of the flow shear parameter, γ_E . Also shown are the 2D mode structures for $\gamma_E = -0.0036$ (c) and $\gamma_E = -0.0090$ (d).

window of existence for the *isolated* mode is very narrow in γ_E . We also show in Figures 3(c) and 3(d) how the eigenmode structure evolves in the poloidal plane from the outboard mid-plane for $\gamma_E = 0$ (Figure 2(a)) to the top of the plasma at $\gamma_E \sim -0.01$. With a positive value of γ_E , the mode moves towards the bottom of the plasma. Adding flow shear to a *general* mode usually has little impact on stability as the mode type does not change, and hence, the averaging procedure used in the ballooning analysis to determine the growth rate is unchanged. The radial width of the mode will, however, be affected because of its dependence on Ω_x .

In conclusion, we have presented numerical 2D eigenmode solutions for micro-instabilities in toroidal geometry. These confirm the analytic asymptotic approaches demonstrated in Refs. 1 and 2. In particular, we find that the common approach to ballooning theory, selecting the value of θ_0 to maximise the growth rate which usually gives rise to a mode that balloons on the outboard side, is only valid in very special situations. More generally, one should average the local (1D ballooning) growth rate over θ_0 , and the dominant mode amplitude will exist off the outboard midplane. Eigenmode frequencies determined from our 2D calculations for a representative model of toroidal drift waves demonstrate excellent agreement with those determined from the 1D ballooning theory, provided one treats θ_0 correctly. Considering the effect of flow shear, we have shown that an *isolated* mode smoothly transforms into the more stable *general* mode as the flow shear is increased, and we have demonstrated the very narrow region of parameter space where the isolated mode exists.

Our analysis is generic to any micro-instability in a tokamak plasma, and may be relevant to situations where plasma gradients, generally clamped by stiff transport from microturbulence, are transiently relaxed by bursty energy releases. In the tokamak high confinement-mode, steep density and temperature gradients form a pedestal close to the plasma edge. The pedestal periodically collapses due to ELMs, with the profiles subsequently rebuilding until the next ELM is triggered. Large ELMs are believed to be due to the onset of intermediate- n ideal MHD peeling-ballooning modes,^{14–16} which become unstable for sufficiently high and wide pedestals. Small ELM regimes are less well understood. The linear growth rate and mode frequency of the high n micro-instabilities responsible for transport in the steep pedestal region, will not typically be stationary at the same location, (x, θ_0) , so that *isolated* modes will not usually exist. Turbulence from the more stable *general* mode will therefore typically constrain the pedestal gradients. As profiles rebuild between ELMs, however, the locations where the frequency and growth rate are stationary also evolve and may transiently become collocated, allowing an *isolated*

mode to exist. At that instant, the gradient would be close to the *general* mode's critical gradient, well above that associated with the *isolated* mode. Therefore the *isolated* mode would suddenly become highly unstable, potentially triggering a rapid crash in the gradients (i.e., a small ELM). Such localised crashes of the pedestal profiles may prevent the equilibrium from ever reaching the ideal MHD instability boundary associated with larger type-I ELMs. This could form the basis of a theory for small ELMs in tokamaks.

The authors gratefully acknowledge helpful discussions with Bryan Taylor and Jack Connor. This work was part-funded by the RCUK Energy Programme under Grant No. EP/I501045 and the European Communities under the contract of Association between EURATOM and CCFE. To obtain further information on the data and models underlying this paper, please contact PublicationsManager@ccfe.ac.uk. The views and opinions expressed herein do not necessarily reflect those of the European Commission.

¹J. B. Taylor, H. R. Wilson, and J. W. Connor, *Plasma Phys. Controlled Fusion* **38**, 243 (1996).

²R. L. Dewar, *Plasma Phys. Controlled Fusion* **39**, 453 (1997).

³J. W. Connor, R. J. Hastie, and J. B. Taylor, *Proc. R. Soc. London, Ser. A* **365**, 1 (1979).

⁴A. H. Glasser in *Proceedings of the Finite beta theory workshop, Varenna*, edited by B. Coppi and W. L. Sadowski (U.S. Dept. of Energy, Washington D.C., 1977), CONF-7709167, p. 55.

⁵R. L. Dewar and A. H. Glasser, *Phys. Fluids* **26**, 3038 (1983).

⁶Y. C. Lee and J. W. Van Dam in *Proceedings of the Finite beta theory workshop, Varenna*, edited by B. Coppi and W. L. Sadowski (U.S. Dept. of Energy, Washington D.C., 1977) CONF-7709167, p. 93.

⁷More generally, this position depends on a number of factors including the surface shaping and instability being considered. In a treatment where both the Ω_{ix} and Ω_x terms are retained, the location of peaking will also depend upon the relative size of these two terms allowing the mode to sit between the two limits obtained by neglecting either of these terms, as demonstrated in Figure 3.

⁸N. Oyama, P. Gohil, L. D. Horton, A. E. Hubbard, J. W. Hughes, Y. Kamada, K. Kamiya, A. W. Leonard, A. Loarte, R. Maingi, G. Saibene, R. Sartori, J. K. Stober, W. Suttrop, H. Urano, W. P. West, and ITPA Pedestal Topical Group, *Plasma Phys. Controlled Fusion* **48**, A171 (2006).

⁹J. W. Connor and J. B. Taylor, *Phys. Fluids* **30**, 3180 (1987).

¹⁰Y. Z. Zhang and S. M. Mahajan, *Phys. Lett. A* **157**, 133 (1991).

¹¹K. Y. Kim and M. Wakatani, *Phys. Rev. Lett.* **73**, 2200 (1994).

¹²R. L. Dewar, Y. Z. Zhang, and S. M. Mahajan, *Phys. Rev. Lett.* **74**, 4563 (1995).

¹³J. W. Connor, R. J. Hastie, and T. J. Martin, in *Proceedings of the International School of Plasma Physics, ISPP21, Theory of Fusion Plasmas, Varenna*, edited by J. W. Connor, O. Sauter, and E. Sindoni (Societa Italiana di Fisica, 2004), p. 457.

¹⁴H. R. Wilson, J. W. Connor, A. R. Field, S. J. Fielding, R. L. Miller, L. L. Lao, J. R. Ferron, and A. D. Turnbull, *Phys. Plasmas* **6**, 1925 (1999).

¹⁵P. B. Snyder, H. R. Wilson, J. R. Ferron, L. L. Lao, A. W. Leonard, T. H. Osborne, A. D. Turnbull, D. Mossessian, M. Murakami, and X. Q. Xu, *Phys. Plasmas* **9**, 2037 (2002).

¹⁶P. B. Snyder, R. J. Groebner, A. W. Leonard, T. H. Osborne, and H. R. Wilson, *Phys. Plasmas* **16**, 056118 (2009).